3988–4000 *Nucleic Acids Research, 2007, Vol. 35, No. 12* *Published online 6 June 2007*
doi:10.1093/nar/gkm419

Effects of nucleoid proteins on DNA repression loop formation in *Escherichia coli*

Nicole A. Becker[1], Jason D. Kahn[2] and L. James Maher III[1,*]

[1]Department of Biochemistry and Molecular Biology, Mayo Clinic College of Medicine, 200 First St SW, Rochester, MN 55905 and [2]Department of Chemistry and Biochemistry, University of Maryland, College Park, MD 20742-2021, USA

Received February 27, 2007; Revised and Accepted May 8, 2007

ABSTRACT

The intrinsic stiffness of DNA limits its ability to be bent and twisted over short lengths, but such deformations are required for gene regulation. One classic paradigm is DNA looping in the regulation of the *Escherichia coli lac* operon. Lac repressor protein binds simultaneously to two operator sequences flanking the *lac* promoter. Analysis of the length dependence of looping-dependent repression of the *lac* operon provides insight into DNA deformation energetics within cells. The apparent flexibility of DNA is greater *in vivo* than *in vitro*, possibly because of host proteins that bind DNA and induce sites of flexure. Here we test DNA looping in bacterial strains lacking the nucleoid proteins HU, IHF or H-NS. We confirm that deletion of HU inhibits looping and that quantitative modeling suggests residual looping in the induced operon. Deletion of IHF has little effect. Remarkably, DNA looping is strongly enhanced in the absence of H-NS, and an explanatory model is proposed. Chloroquine titration, psoralen crosslinking and supercoiling-sensitive reporter assays show that the effects of nucleoid proteins on looping are not correlated with their effects on either total or unrestrained supercoiling. These results suggest that host nucleoid proteins can directly facilitate or inhibit DNA looping in bacteria.

INTRODUCTION

DNA looping has been proposed as a fundamental mechanism for action at a distance in the control of gene expression and DNA recombination [reviewed in (1)]. It is of interest to understand whether the intrinsic physical properties of DNA are consistent with DNA looping constrained only through protein binding at the ends of the loop, or if looping also requires the action of proteins that enhance the apparent flexibility of the intervening DNA. There is active debate over the best model for describing local DNA stiffness, including recent controversial results on the probability of large bends in short pieces of DNA (2–6). However, it is clear from *in vitro* experiments that DNA strongly resists bending and twisting over distances shorter than its ~150 bp persistence length. For example, the efficiency of *in vitro* recombination using the *Hin* invertasome system falls dramatically as the length of DNA looped between recombination sites is reduced below one persistence length (7). That this effect is due to bending stiffness is confirmed by the observation that restriction fragments shorter than ~200 bp are poor substrates for cyclization by DNA ligase (8). Both reactions involve contact between distant DNA sites, and their rates are both increased dramatically when sequence-non-specific architectural proteins (bacterial HU or eukaryotic HMGB proteins, respectively) are present. Architectural binding proteins are sequence-specific or non-specific proteins whose main functions appear to be reshaping DNA and/or changing its apparent stiffness (9–20). Despite considerable study, it remains unclear whether these proteins function to increase apparent flexibility by creating static bends at various locations or by inducing flexible DNA kinking. The lifetimes of many such complexes on unperturbed DNA are unknown.

Both prokaryotes and eukaryotes must dramatically compact their genomic DNA while maintaining access of the genetic material to replication, transcription and repair machinery. If it were rigid, the 4.5×10^6 bp *E. coli* chromosome would form a circle 1.5 mm in circumference. The intrinsic flexibility of DNA should allow spontaneous collapse only to a volume of ~200 μm^3 (i.e. ~400 times larger than the *Escherichia coli* nucleoid). Thus, significant further DNA compaction must be achieved *in vivo* (21). Proteins can facilitate this additional compaction using binding-free energy available from protein/DNA interactions. Genome compaction in eukaryotes is achieved by the spooling of DNA onto histone octamers and packing of the resulting nucleosomes into 30 nm and higher-order

*To whom correspondence should be addressed. Tel: 507 284 9041; Fax: 507 284 2053; Email: maher@mayo.edu

fibers. Packaged prokaryotic DNA lacks defined structures analogous to nucleosomes. Rather, six key nucleoid proteins assemble with the bacterial chromosome (21–23). These proteins include (in decreasing order of abundance during exponential growth): factor for inversion stimulation (Fis), heat-unstable nucleoid protein (HU), integration host factor (IHF), histone-like, nucleoid-structuring protein (H-NS), suppressor of td mutant phenotype A (StpA) and DNA-binding protein from starved cells (Dps). The present work focuses on HU, IHF and H-NS.

HU is a heterodimer of 90-residue (9.2 kDa) HU-1 and HU-2 subunits encoded by the *E. coli hupA* and *hupB* genes, respectively (22,24). HU binds DNA without sequence specificity, but has been reported to bind with greater avidity to pre-bent or kinked DNA (25–28), consistent with expectations for a DNA-bending protein. HU accumulates to ~25 000 dimers per cell during exponential growth, and it has been proposed that the protein functions in many processes including DNA replication, transcriptional repression and recombination (23). HU facilitates formation of a DNA repression loop in the *gal* operon, where the protein reportedly binds a specific sequence in the loop (29). Analysis of co-crystals of HU and DNA show sharp and variable DNA bending around the protein (30).

The integration host factor IHF, named for its role in phage λ integration, binds specific asymmetric DNA sites (WATCAANNNNTTR; W, A or T; N, any base; R, A or G) as a heterodimer (31,32), bending DNA by 160°. IHF and HU monomers share ~30% sequence identity and are related in both structure and function (20,31,33). The IHFα (99 aa, 11.2 kDa) and IHFβ (94 aa, 10.7 kDa) subunits are ~30% identical to each other (and to HU monomers) and are encoded by the *E. coli himA* and *himD* genes, respectively. Unlike HU, which can form either homodimers or heterodimers, IHF is isolated from cells only as a heterodimer, and IHFβ homodimers can only be produced at high subunit concentration *in vitro*. Such IHFβ homodimers bind DNA with 100-fold lower affinity than heterodimers, and IHFα homodimers are even less stable; thus, the removal of only the IHFβ subunit in our experiments should eliminate all DNA-binding activity (34). Cells contain ~10 000 IHF dimers during exponential growth (23). Gene array profiling indicates that the expression of at least 100 genes is altered upon deletion of IHF, with 46 of the genes containing putative IHF-binding sites (35).

H-NS homodimers (137 aa, 15.4 kDa), the product of the *E. coli hns* gene, also accumulate to ~10 000 dimers per cell (21,36,37). The protein is believed to oligomerize into higher-order complexes via a coiled-coil domain (23,38,39). The protein C-terminus binds DNA, appearing to prefer A/T-rich or curved DNA. H-NS acts as a transcriptional repressor or silencer, with an H-NS-deficient strain showing increased expression of >100 genes (39). H-NS protein may be involved in DNA condensation, and overexpression is lethal (24,40–43). The H-NS-like Sfh protein carried by R27 plasmids of *Salmonella typhimurium* (44) appears to act as a general repressor of plasmid transcription, as the plasmid is better tolerated by the host in the presence as opposed to the absence of Sfh. This result suggests a general role of H-NS-like proteins in gene repression.

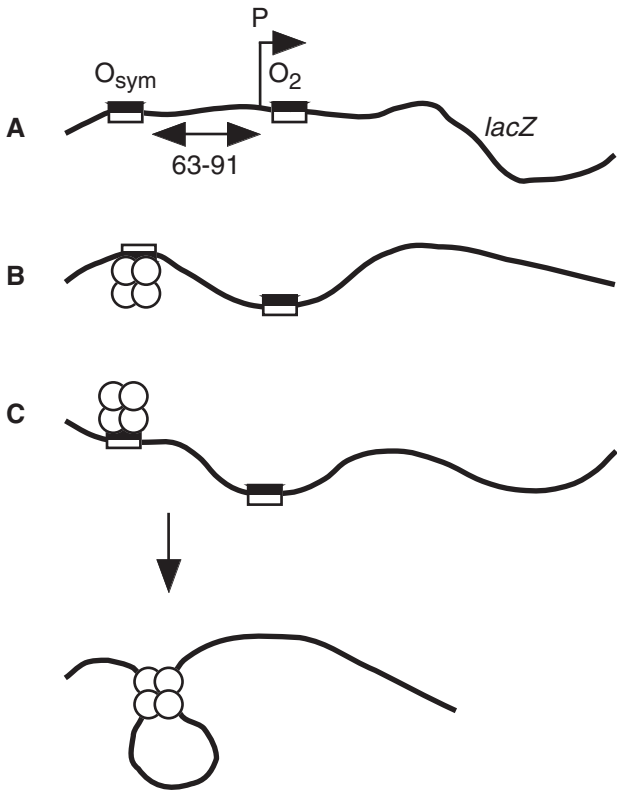

Figure 1. *In vivo* DNA looping assay. (**A**) Arrangement of strong (O_{sym}) and weak (O_2) *lac* operators (rectangles) flanking the *lac* promoter (P) upstream of the *lacZ* reporter gene. Operator spacing was systematically varied from 63 to 91 bp in individual strains. The binding face recognized by repressor tetramer is indicated by shading. (**B**) The Lac repressor tetramer (circles) fills the high-affinity O_{sym} operator, but repression by looping to the O_2 operator depends on the properties of the intervening DNA. Looping is disfavored by the energetic costs of twisting and bending DNA. Spacings that position operators on opposite faces of the DNA helix are unfavorable for repression loops because of the requirement for DNA twisting. (**C**) Spacings that position operators on the same face of DNA are favorable for repression loop formation.

We have developed an experimental system for measuring DNA flexibility in living *E. coli* cells and have used it to determine whether proteins play important roles in enhancing the apparent flexibility of DNA. The system, shown schematically in Figure 1, is based on classic studies of DNA looping in repression of the *E. coli* lactose operon (45–48). The reporter construct is a simplified *lac* operon, with a *lacZ* reporter gene placed downstream from the moderately strong *lac* UV5 promoter. The operon is modified so as to increase sensitivity to DNA looping by using a weak proximal O_2 operator to mediate repression and a strong distal O_{sym} operator upstream. The Lac repressor binds strongly to O_{sym}, and it can form a repression loop by simultaneously binding at O_2. The stability of this loop is related to the energetic costs of bending and twisting the intervening DNA, which are, in turn, dependent on the distance of separation and helical phasing of the operators. The reporter is introduced in

single copy on an F′ episome. Host strains with or without the genes encoding architectural DNA-binding proteins are used; they all express wild-type levels of the wild-type bidentate Lac repressor tetramer (49). The development of this system and its application to flexibility induced by the rat HMG-B protein have been described in detail (49).

Measurement of the degree of promoter repression as a function of operator separation provides information about the longitudinal and torsional bending properties of DNA *in vivo*. Control experiments using IPTG (a stable allolactose analog) reveal the behavior of the system when the affinity of repressor for DNA has been dramatically reduced. Previous characterization of this system for loop lengths of 63–91 bp revealed that (i) DNA twisting rather than bending is the major obstacle to DNA looping; (ii) weak repression loops are still detected in the presence of saturating concentrations of IPTG; (iii) deletion of the *E. coli* architectural protein HU dramatically destabilizes repression loops; (iv) replacement of *E. coli* HU with heterologous mammalian HMGB proteins can partially rescue DNA looping and (v) the effect of HU loss on DNA looping does not result from changes in DNA supercoiling (49). The key conclusion of these experiments was that the sequence-non-specific HU protein is required to stabilize small repression loops *in E. coli*.

These data as well as the original length-dependence work of Müller-Hill (48) have been analyzed recently by others, using several different formalisms (50). In one analysis (50) it was concluded that the bending properties of DNA in cells lacking HU match those measured *in vitro*, but other work has used Lac operon looping to support the existence of surprisingly easily bent DNA (1). An earlier rod mechanics model of the loop suggested that the repressor conformation changes depending on the supercoiling environment (51), in agreement with earlier experiments (52). The additional repression peaks caused by weak loops formed by the presence of IPTG-bound repression [conclusion (ii) above] have been identified in the Müller-Hill data set (48,53). Clearly, more experimental work is needed to clarify the loop geometry, the dependence of DNA flexibility on architectural proteins, and the effects of supercoiling.

The present study explores how the loss of HU and other *E. coli* nucleoid proteins affects DNA looping. We have confirmed and extended our earlier results. The most surprising new finding is that H-NS acts to destabilize rather than stabilize small loops. Changes in either total or unrestrained superhelicity do not appear to explain the effects of architectural proteins on DNA looping.

MATERIALS AND METHODS

Bacterial strains and gene disruption

E. coli strains bearing gene disruptions are described in Table 1. The *hupA* and *hupB* genes were disrupted in parental *E. coli* strain FW102 (54) as described (49,55). Disruption of the *himD* gene (encoding the IHFβ subunit) was accomplished by gene-targeted recombination with a kanamycin selectable marker (complementary sequence in bold) amplified with primer pair LJM-2485 5′-$A_2TCA_2TGCAGCA_2CAGCAGC_2GCT_2A_2T_3GC_2T_3$ $A_2G_2A_2C_2$**$GTGTAG_2CTG_2AGCTGT_2C$** and LJM-2486 5′-$A_6GCAC_3GACAG_2TGCT_4CTCTCGT_2CA_2GT_3GA$ GTA**$AT_2C_2G_4ATC_2GTCGAC_2$** by published methods (55). Disruption of the *hns* gene similarly involved recombination with a selectable marker (complementary sequence in bold) amplified with primer pair LJM-2477 5′-$TA_2G_2CTCTAT_2ACTAC_4A_2CA_3C_2AC_4A_2TATA_2GT_3$ G**$GTGTAG_2CTG_2AGCTGCT_2C$** and LJM-2478 5′-AT $A_6TC_2GC_2GCTG_2CG_3AT_4A_2GCA_2GTGCA_2TCTAC$**A** **$T_2C_2G_4ATC_2GTCGAC_2$**. In each case, the integrated selectable marker was removed in a second step involving recombination between FRT sites as described (55). Genotypes of all deletion strains and the presence of looping assay episomes were confirmed by diagnostic PCR amplification following conjugation and selection.

In vivo DNA looping assay

DNA looping constructs were based on plasmid pJ992, created by modifications of pFW11-null (54) as previously described (49). Constructs contained a strong distal O_{sym} operator and a weak proximal O_2 operator. The O_2 operator normally present within the *lacZ* coding region was destroyed by site-directed mutagenesis (49). A construct with a proximal O_2 but lacking upstream O_{sym} was used as a normalization control. Test promoters did not contain CAP-binding sites. *lacZ* looping constructs were placed on the single copy F128 episome by homologous recombination between the constructed plasmids and bacterial episome. F128 carries the *lacI* gene producing wild type levels of repressor. Bacterial conjugation and selections were carried out as previously described (54). After mating and selection, correct recombinants were confirmed by PCR amplification.

Reporter assay

All chemicals were obtained from Sigma (St Louis, MO, USA). *lacZ* expression was measured by a liquid β-galactosidase colorimetric enzyme assay as

Table 1. Bacterial strains disrupted in genes encoding nucleoid proteins

Strain	Relevant genotype	Designation	Comment
FW102[a]	$Strep^R$ derivative of CSH142 [*araD*(*gpt-lac*)$_5$]	WT	
BL643	FW102 Δ*hupA* Δ*hupB*	ΔHU	Loss of both HU-1 and HU-2 subunits of HU heterodimer
BL706	FW102 Δ*hns*	ΔH-NS	Loss of H-NS homodimer
BL707	FW102 Δ*himD*	ΔIHF	Loss of IHFβ subunit of IHF heterodimer. IHFα homodimers are not stable.

[a]FW102 was the kind gift of F. Whipple. BL strains were created for this study.

described (56). The assay was modified as follows to increase efficiency: cultures were grown in 1.1 ml LB/antibiotic in 96-well boxes (2 ml capacity per well) with shaking (250 rpm) at 37°C. Subcultures (1.1 ml of media) were then inoculated with 30 µl of overnight culture in the presence or absence of 2 mM IPTG. Subcultures were grown with shaking at 37°C until OD_{600} reached ~0.3. For samples with low β-galactosidase activity, 800 µl of bacterial culture was assayed after centrifugation and resuspension in 1 ml Z-buffer (60 mM Na_2HPO_4, 40 mM NaH_2PO_4, pH 7.0, 10 mM KCl, 1 mM $MgSO_4$, 50 mM β-mercaptoethanol). For samples with high levels of β-galactosidase activity, 100 µl of bacterial culture was diluted with 900 µl of Z-buffer before analysis. Cells were lysed by addition of 50 µl chloroform and 25 µl 0.1% SDS, followed by repeated pipetting (10–12 times) with a 12 channel pipettor. Samples were equilibrated at 30°C for 5 min, followed by the addition of 200 µl of 4 mg/ml O-nitrophenylpyranogalactoside (ONPG) in Z-buffer. Incubation at 30°C continued with accurate timing until OD_{420} reached ~0.5. Reactions were stopped with 500 µl 1 M Na_2CO_3 and the reaction time was recorded. Cell debris was pelleted by centrifugation of the 96-well box for 10 min at 4000 × *g*. Three hundred and fifty microliters of cleared samples were transferred to 96-well plates. Sample OD readings were measured on a Molecular Devices SpectraMax 340 microtiter plate reader. β-galactosidase activity (*E*) was calculated according to:

$$E = 1000\frac{[OD_{420} - 1.75(OD_{550})]}{t \bullet v \bullet OD_{600}} \quad \mathbf{1}$$

where OD_x refers to optical density at wavelength *x*, *t* is the reaction time (min) and *v* is the assay culture volume (ml). Assays were performed with a total of six colonies from each independent strain repeated on two different days.

Looping data analysis and modeling

The enhancement of repression due to specific DNA looping is expressed in terms of the normalized expression parameter E', according to:

$$E' = \frac{E_{OsymO2}}{E_{O2}} \quad \mathbf{2}$$

where E_{OsymO2} is the raw β-galactosidase activity (induced or uninduced) from test constructs with both O_{sym} and O_2 operators, and E_{O2} is the corresponding raw β-galactosidase activity (induced or uninduced) from test constructs with only the proximal O_2 operator. Note that Equation 2 is corrected from the original report (49).

The conventional repression ratio, *RR*, is given by

$$RR = \frac{E_{+IPTG}}{E_{-IPTG}} \quad \mathbf{3}$$

where *E* is the raw β-galactosidase activity under the indicated conditions.

A previously described statistical weights/DNA mechanics model (49) was used for simultaneous fitting of experimental E' and *RR* data to expressions for the distribution of possible states of the O_2 operator under repressed and induced conditions. The experimentally derived fraction of O_2 that is bound by repressor (f_{bound}) is modeled as a function of DNA spacer length (*sp*) with five adjustable parameters: the optimal operator spacing in bp ($sp_{optimal}$), the DNA helical repeat (*hr*), the apparent torsional modulus of the DNA loop (C_{app}), the equilibrium constant for specific O_{sym}–O_2 loop formation when operators are perfectly phased (K_{max}) and an equilibrium constant for non-specific looping (K_{NSL}). The K_{NSL} term describes all forms of O_{sym}-dependent enhanced binding to O_2 other than the specific loop; for example, it could include looping between O_{sym} and a pseudooperator overlapping O_2, or enhanced O_2 binding via sliding or hopping from O_{sym}.

Assay of total supercoiling

The total linking number deficit of plasmid DNA isolated from cells (500 ng) was assayed by separating topoisomers on multiple agarose gels at different concentrations of chloroquine (49,57). Electrophoresis was performed at 2 V/cm for ~18 h in 1X TAE buffer (40 mM Tris–acetate and 1 mM EDTA) through 0.8% agarose gels containing 0–10 µg/ml chloroquine. Gels were then stained with 0.5 µg/ml ethidium bromide until bands were barely visible, nicked for 30 s with long-wave UV irradiation, and then stained for an additional 30 min prior to photography. This procedure assures that the ethidium bromide binds equivalently to the different topoisomers.

Assays of unrestrained supercoiling

Trimethylpsoralen (TMP; Sigma) photo-crosslinking of plasmid DNA followed by Southern analysis was performed with modifications of a published method (58). Briefly, bacterial strains containing plasmid pJ992 (49) were subcultured and grown to mid-log phase, $A_{600} \sim 0.6$, typically in 5 ml of LB medium containing antibiotics. Cultures were pelleted by centrifugation at 3000 × *g* for 10 min, washed in M9 salts (56) and resuspended in M9 salts at 1/10 of the original volume, all at 4°C. TMP treatment and the initial steps of DNA harvesting were performed in the dark at 4°C unless otherwise indicated. An ethanol-saturated solution of TMP (5 µl) was added to 500 µl cell culture in a 6-well plate and allowed to equilibrate for 5 min. Samples were irradiated for various times using long-wavelength UV light (~366 nm) delivered from a hand-held (Mineralight) lamp at an intensity of 0.6 mW/cm^2. To compensate for TMP autoinactivation, additional TMP was added every 10 min (59). Cells were then lysed and DNA harvested as previously described (58). DNA was digested with *Xma*I to yield an ~950 bp restriction fragment from plasmid pJ992. A sample (5 µg) of the total resulting DNA was denatured in 100 mM NaOH by treatment for 2 min at 55°C followed by acid neutralization, and electrophoresed on a 1.2% agarose gel at 3 V/cm (60). DNA was transferred to a Nytran membrane (Whatman) using an alkaline transfer system following the manufacturer's recommended protocol. After UV cross-linking to the membrane

(Stratalinker apparatus), the membrane was hybridized with a radioactive probe specific for the DNA fragment of interest. The hybridization signal was quantitated using a Molecular Dynamics Storm PhosphorImager.

Plasmids pJ1345 (original name pPHB94) and pJ1346 (original name pPHB95) are derived from previously described constructs (61) and were the generous gifts of P. Heisig. Plasmid pJ1345 contains the luciferase gene under control of the *topA* promoter cluster, while plasmid pJ1346 places the same reporter under the control of the *gyrA* promoter (Figure 4). For comparisons of unrestrained supercoiling strain in different genetic backgrounds, the *topA* promoter cluster and *gyrA* promoter were assayed in two additional contexts. Plasmids pJ1454 and pJ1456 place the promoters on pJ992, a smaller pACYC184-based plasmid for comparison (49,54). Primers 5′-$CGAC_2G_2ATC_2T_2ATC_2GTACTC_2TGATG$ and 5′-$GCTCGCTGCAGCG_2TGAGA_2TG_2CA_4G$) were used to amplify the promoter and reporter regions from plasmid pJ1345 (~2300 bp product) and pJ1346 (~2000 bp product), installing flanking *BamH*I and *Pst*I restriction sites. PCR products were cloned between the *BamH*I and *Pst*I restriction sites of pJ992 to create plasmid pJ1454 (luciferase gene under the control of the *topA* promoter) and plasmid pJ1456 (luciferase gene under the control of the *gyrA* promoter). The promoter-reporters from pJ1454 and pJ1456 were also moved onto the single copy F128 episome by homologous recombination (54). Luciferase assays were performed using the Promega Luciferase assay kit with modifications to accommodate bacterial cells. Briefly, subcultures (5 ml) in LB media containing kanamycin were inoculated with saturated overnight culture (125 µl). Subcultures were grown at 37°C, with agitation, until A_{600} reached ~0.6. A sample of the culture (90 µl) was combined with buffer (10 µl: 1 M K_2HPO_4 pH 7.8, 20 mM EDTA). Samples were mixed and frozen at −80°C for 30 min. To each thawed sample, cell culture lysis reagent (200 µl; Promega, Madison, WI) and fresh lysozyme mix (100 µl of solution containing 5 mg/ml lysozyme and 5 mg/ml BSA) was added. Samples were incubated at 25°C for 10 min. Accurately measured samples (1–5 µl) were added to luminometer tubes followed by the addition of luciferase assay reagent (100 µl; Promega) and luciferase activity was measured on a Turner 20/20 luminometer. The normalized unrestrained supercoiling ratio (*Qsc*) is given by the *topA*: *gyrA* reporter expression ratio, after normalization for cell density:

$$Qsc = \frac{A'_{topA}}{A'_{gyrA}} \quad \mathbf{4}$$

where A′ is the number of light units per OD600 of culture, and subscripts *topA* and *gyrA* refer to the promoters of the *luc* reporter genes.

RESULTS AND DISCUSSION

DNA looping in the presence of all nucleoid proteins

We first collected expression data for the full set of operator spacings using recombinant F′ episomes carried in our standard laboratory strain of *E. coli* (FW102, labeled 'WT'). Data are shown in Figure 2A. The upper panel displays the conventional repression ratio (*RR*), while the lower panel shows normalized expression (*E′*) both in the absence and presence of 2 mM IPTG as inducer. Data points were analyzed by a statistical weights/DNA mechanics model (49) with simultaneous fitting to *RR* and *E′* data. The full data set is given in Supplementary Tables S1 and S2, and curve fit parameter estimates are provided in Table 2. Since our previous work, we introduced assay modifications that allow more rapid data collection and therefore more simultaneous measurements directly comparing different strains and conditions. The changes in assay timing, however, resulted in slightly higher measurements of gene expression for the most tightly repressed WT strains. Even so, the fit parameters in Table 2 for WT cells are quite similar to the previous report (49). The value for K_{max} is slightly smaller reflecting less-efficient peak repression and the value of K_{NSL} is slightly larger to compensate for the largely unchanged level of out-of-phase repression. All data reported here are new and were collected using the same methodology.

The repression ratio data for WT cells are characterized by periodic oscillation, with peaks (maximal repression) corresponding to alignment of operators on the same DNA face separated by integral multiples of the helical repeat of the DNA. As previously noted (49), the oscillation pattern contains secondary peaks, and it also appears to be damped as DNA length increases. The origin of this unexpected complexity is revealed by plotting the *E′* data from both induced and uninduced WT cells (Figure 2A, lower panel). It is clear that under both conditions reporter expression oscillates with the DNA helical repeat, but that the oscillations are not precisely in phase. This is evidence for weak looping by Lac repressor even under conditions of induction at saturating IPTG concentrations. Optimal operator spacing differs by ~0.5 bp and the helical repeat differs by ~0.9 bp when loops are fit under induced versus uninduced conditions (Table 2). The complex peak structure of the repression ratio curve reflects dephasing (due to the helical repeat difference) between the uninduced and induced *E′* data rather than a spacing-dependent change in DNA looping energy. The apparent overall damping in the repression ratio is also due to dephasing, as well as to broadening of the torsional oscillations as the length increases. It does, however, appear that points at longer DNA length tend to fall slightly below the fit curves, suggesting a weak effect of longitudinal flexibility. This lack of a strong dependence of optimal loop probability on DNA length for such small DNA segments suggests enhanced apparent DNA longitudinal flexibility *in vivo*: if the loop-free energy were controlled by the *in vitro* DNA elastic bending energy, we would have observed much more dramatic length dependence. The low fit value of the apparent DNA torsional modulus (C_{app}; Table 2) suggests a similar increase in apparent torsional flexibility.

DNA looping in the absence of HU, IHF or H-NS

Analysis of the ΔHU *E. coli* strain (Figure 2B) substantiates previous observations that loss of HU substantially disables looping (49). The observed ~3-fold effects of genetic background on promoter strength are factored out of both repression ratio (upper panel) and E' data (lower panel), so Figure 2 reflects specific effects on DNA loop stability. Loss of HU protein causes a global ~3-fold promoter derepression (Figure 2B), reflected in a ~3-fold decrease in estimated equilibrium constants for specific and non-specific loop formation (K_{max} and K_{NSL}, Table 2). Notably, induced *lacZ* expression shows almost no residual operator phase dependence (Figure 2B, lower panel, filled circles), suggesting that the putative loop formed by IPTG-bound repressor requires HU for stability. The optimal operator spacing for uninduced DNA looping is ~2 bp shorter in the absence of HU, suggesting a change in the optimum repression loop geometry, a reorganization of the DNA domain, or a change in the local supercoiling status in the absence of this nucleoid protein. Destabilization of DNA looping in the absence of HU could imply a direct, sequence-non-specific but possibly structure-specific binding of HU to looped DNA, as is seen for the related Gal

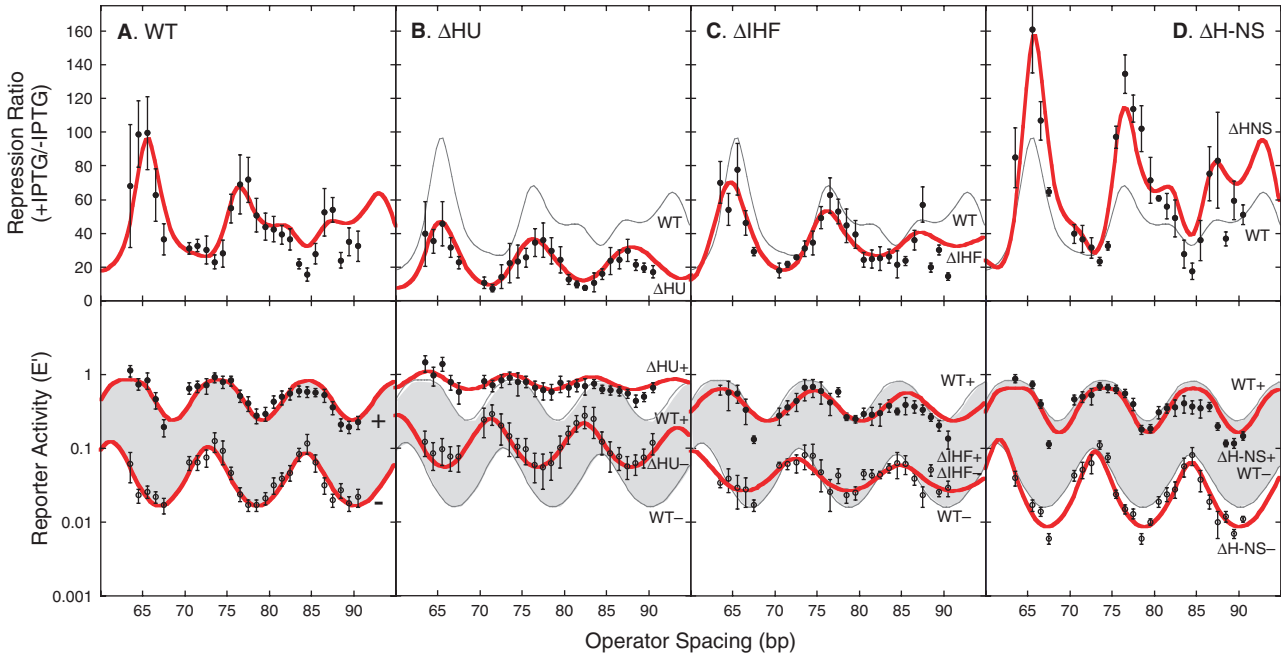

Figure 2. Dependence of DNA looping on nucleoid proteins. *RR* (upper panels) and E' (lower panels) parameters were calculated as described in 'Materials and Methods' section. Closed and open symbols in lower panels reflect data obtained in the presence and absence of IPTG, respectively. Mean and standard deviation reflect assays from six different colonies repeated on two different days. Panels (**A**–**D**) show expression data reflecting DNA looping in (**A**) WT *E. coli,* (**B**) cells lacking HU, (**C**) cells lacking IHF and (**D**) cells lacking H-NS. Each new data set is shown as mean with standard deviations. Least squares curve fits (red) are based on the statistical weights/DNA mechanics model with simultaneous fitting to *RR* and E' data. The fits to the WT data from A are replicated in panels B–D in gray with thin lines, for comparison. Shading between uninduced and induced WT E' fits (lower panels) is to facilitate comparison.

Table 2. Fitting parameters from statistical weights/DNA mechanics model of DNA looping[a,b]

Strain	$sp_{optimal}$ (bp)[c]		C_{app} ($\times 10^{-19}$ erg cm)[d]		*hr* (bp/turn)[e]		K_{max}[f]		K_{NSL}[g,h]	
IPTG	–	+	–	+	–	+	–	+	–	+
WT	78.7 ± 0.2	79.2 ± 0.3	0.73 ± 0.14	1.16 ± 0.52	11.6 ± 0.3	10.7 ± 0.4	211 ± 99	2.6 ± 0.1	20.3 ± 0.6	0 ± 0.8
ΔHU	76.9 ± 0.6	78.6 ± 0.7	0.68 ± 0.11	0.33 ± 0.08	11.1 ± 0.3	9.7 ± 0.6	65 ± 11	1.6 ± 0.6	8.4 ± 5.4	0 ± 1.7
ΔIHF	78.8 ± 0.5	80.3 ± 0.5	0.40 ± 0.07	0.67 ± 0.33	12.4 ± 0.7	11.1 ± 0.6	87 ± 19	2.0 ± 1.0	(8.4) ± 61	0 ± 0.7
ΔH-NS	77.0 ± 0.2	79.0 ± 1.3	0.69 ± 0.09	1.38 ± 0.60	11.4 ± 0.3	10.6 ± 0.4	359 ± 199	3.0 ± 1.6	(8.0) ± 38	0 ± 1.0

[a]The indicated error range are the 95% confidence limits from Matlab.
[b]The fits are to E_{+IPTG}, E_{-IPTG} and *RR* simultaneously.
[c]Operator spacing (center-to-center) nearest 80 bp for optimal DNA loop stability.
[d]Apparent torsional rigidity of the protein/DNA loop (compare with value for DNA *in vitro*: 2.3–3 × 10^{-19} erg cm).
[e]DNA helical repeat (bp/turn).
[f]K_{max} = [specific DNA loop]/[free operator] for the most stable loop at the cellular [LacI], assumed to be constant.
[g]K_{NSL} = [$\sum$(non-specific DNA loops)]/[free operator].
[h]Parentheses indicate an unreliable parameter estimate (large error).

repressor (62). An alternative, though not mutually exclusive, possibility is that unrestrained negative superhelical strain in this region of the F′ element stabilizes DNA looping and loss of HU reduces this strain.

Looping assays in cells lacking the sequence-specific nucleoid protein IHF show only a modest looping disability relative to WT cells (Figure 2C). Residual repression under inducing conditions is marginally decreased relative to WT. The phase-dependence of repression in the absence of IPTG is slightly reduced (reflected in a smaller C_{app}), and the equilibrium constant K_{max} for the most stable loop is ~2-fold reduced in the absence of IHF (Table 2). IHF protein displays both sequence-specific and non-specific binding (21), and the experimental DNA looping constructs do not contain specific IHF recognition sequences. These results suggest that non-specific IHF binding contributes only slightly to apparent DNA flexibility under these conditions.

Cells that do not produce H-NS protein were also tested. Quite surprisingly, ΔH-NS cells showed substantially *improved* DNA looping compared to WT *E. coli* (Figure 2D). Repression ratios were ~2-fold improved for optimally aligned operators, while remaining unchanged for operators on opposite helical faces of DNA. These effects are also clear in the E' data (Figure 2D, lower panel) where troughs (maximal repression in the absence of IPTG; open circles) are deepened in the absence of H-NS, while peaks (promoter leakiness with out-of-phase operators) are unchanged. Upon H-NS deletion, stabilization of the optimally aligned loop is most apparent, reflected in the model fitting parameters by a ~1.7-fold increase in the looping equilibrium constant K_{max}. For out-of-phase operators the corresponding stabilization is not observed due to the disappearance of significant nonspecific looping (a decrease in K_{NSL} from ~20 to ~0). We caution that the K_{NSL} parameter is often not precisely determined by the data, so our interpretations do not rest on it. Finally, upon H-NS deletion C_{app} remains essentially the same, suggesting that H-NS does not change the twist flexibility of DNA significantly: in the context of the weak induced loop the protein may increase twist flexibility very slightly.

These results suggest that the presence of H-NS primarily acts to destabilize DNA looping through its effect on DNA bending, not twisting. This loop destabilization could be due to decreasing the longitudinal flexibility of DNA, but we do not observe a progressive change in the peak and trough heights with length, as might be expected in this case. H-NS could also constrain the DNA in a conformation that tends to prevent looping, as discussed later. Overall, the changes in the K_{max} and K_{NSL} parameters suggest that H-NS constrains the DNA in some fashion that allows (or perhaps even enhances) non-specific contacts between DNA sites but tends to destabilize the specific O_{sym}–O_2 loop.

It is quite surprising that loss of one nucleoid protein (HU) disables DNA looping, while loss of another (H-NS) facilitates DNA looping. One obvious possibility is that these effects are due to changes in local or global supercoiling, and this was investigated in further experiments.

Role of unrestrained negative supercoiling in DNA looping

Perturbations in the normal complement of nucleoid proteins could influence the stabilities of repression loops by direct and/or indirect mechanisms. For example, direct loop stabilization could occur if architectural proteins bind within the DNA loop so as to introduce at least transient favorable bends or sites of flexibility. Indirect effects on DNA looping could result from local changes in superhelical strain or superhelix geometry caused by the absence of a nucleoid protein. To differentiate among explanations invoking superhelical writhe, twist strain and protein binding, it is important to have measurements of *restrained* supercoiling (due to DNA wrapping on protein surfaces), and *unrestrained* supercoiling, which creates actual mechanical twisting strain (63). The total DNA linking number deficit is the sum of these two components. Restrained supercoiling could be important in creating a DNA geometry favorable or unfavorable for looping, whereas unrestrained supercoiling has the potential to drive the compaction of naked DNA, facilitating formation of the repression loop. Enhancement of DNA looping by supercoiling has been reported *in vitro* (64–66) and *in vivo* (29).

To determine whether direct or indirect mechanisms better explain the effects of nucleoid proteins on DNA looping, we independently measured both total and unrestrained negative supercoiling in WT, ΔHU, ΔIHF and ΔH-NS *E. coli* strains using several methods. Total supercoiling was monitored by assessing plasmid topoisomer distributions after extraction from cells, using electrophoretic separation of topoisomers in agarose gels containing different concentrations of the intercalating agent chloroquine. The concentration of chloroquine required to alter DNA twist sufficiently to eliminate negative supercoils (thereby maximally reducing plasmid electrophoretic mobility) is directly related to the initial negative superhelical density of the extracted plasmid. Figure 3 and Table 3 show the results when plasmids from WT, ΔHU, ΔIHF and ΔH-NS strains were electrophoresed in the presence of 1, 2, 3, 5, 7 or 9 μg/ml chloroquine. Plasmid topoisomer mobility decreased over this chloroquine concentration range, demonstrating that all plasmid populations were initially negatively supercoiled. Importantly, however, the degree of total negative supercoiling depended on the complement of nucleoid proteins. Inspection of the electrophoresis series showed that total negative supercoiling was indistinguishable in WT and ΔH-NS strains. In contrast, total negative supercoiling was strongly reduced in ΔHU cells but strongly increased in ΔIHF relative to WT (this is most clear Figure 3, 7 μg/ml chloroquine). The result for ΔHU cells confirms our previous observations (49).

As discussed earlier, the chloroquine titration method assays total supercoiling, reflecting the *in vivo* sum of restrained and unrestrained supercoiling of plasmids in the cell. Because unrestrained supercoiling generates local twisting strain, while restrained supercoiling does not, it was important to determine if levels of unrestrained supercoiling follow the same trends as those seen in Figure 3.

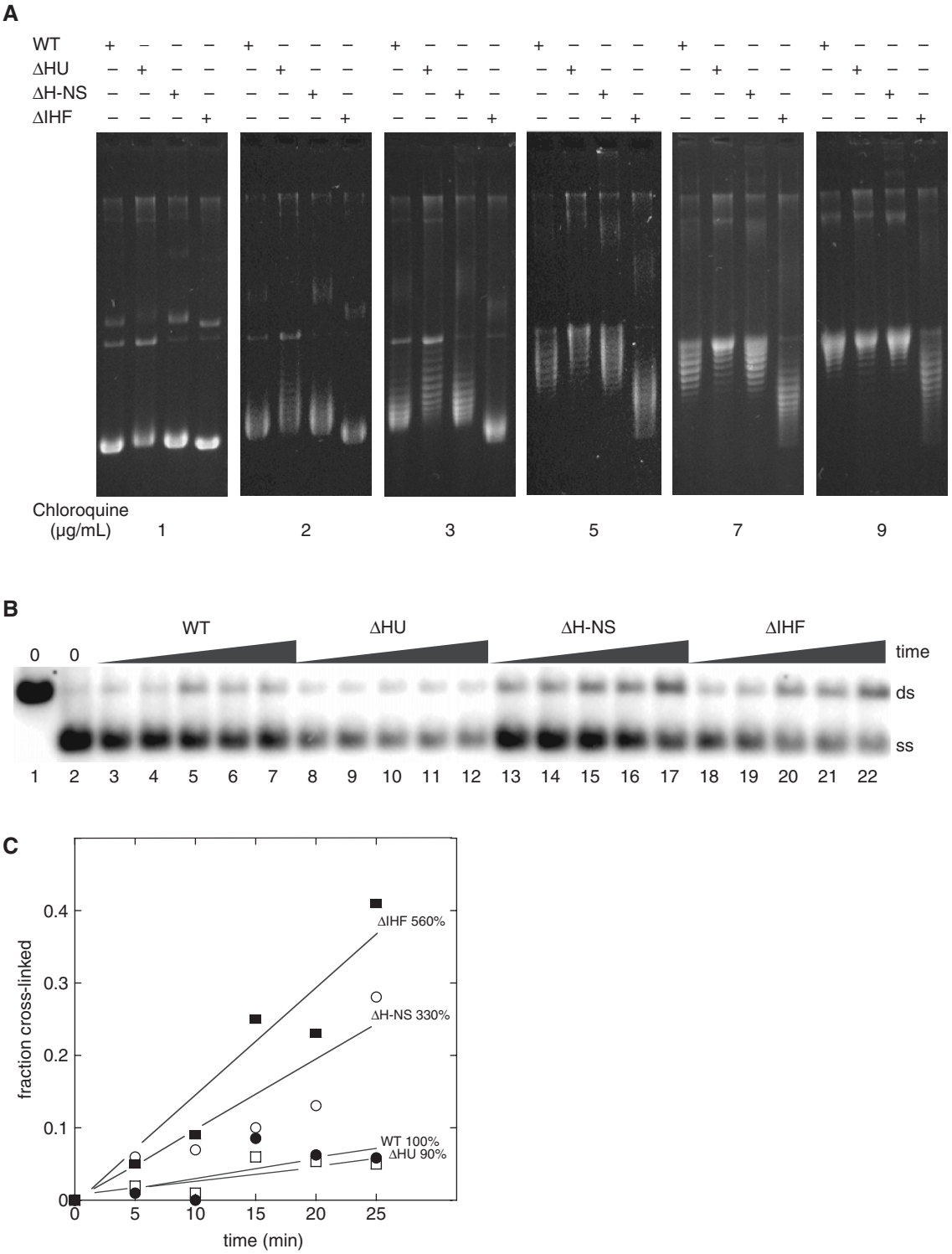

Figure 3. Effects of nucleoid proteins on DNA supercoiling. (**A**) Effects on total supercoiling. The superhelical strain in plasmid pJ1035 isolated from the indicated *E. coli* strains was measured by electrophoresis in the presence of the indicated concentrations of the weak intercalator chloroquine, as described in 'Materials and Methods' section. Negatively supercoiled plasmid DNA (high mobility) is relaxed by increasing binding of chloroquine over this range of concentrations. (**B**) Unrestrained superhelical strain is measured by the rate of psoralen crosslinking of plasmid DNA. The Southern blot distinguishes ssDNA and rapidly renaturing dsDNA. Native (lane 1) and denatured (lane 2) markers are shown. Cross-linked (ds) and non-cross-linked (ss) mobilities are indicated. Samples were analyzed after 5, 10, 15, 20 or 25 min of exposure to TMP in WT (lanes 3–7), ΔHU (lanes 8–12). ΔH-NS (lanes 13–17) and ΔIHF (lanes 18–22) cells. (**C**) Quantitation of data from panel B after subtraction of local background signal. WT: filled circles; ΔHU: open squares; ΔH-NS: open circles; ΔIHF: filled squares. The percentages indicated are the slopes fit by linear regression relative to the WT slope.

One biochemical approach to the measurement of unrestrained supercoiling *in vivo* was developed for eukaryotic cells. It is based on the enhanced binding and photocrosslinking of intercalating psoralen derivatives to DNA under unrestrained superhelical strain (67). We adapted this approach to monitor changes in superhelical strain in prokaryotes. The assay measures changes in the rate of trimethylpsoralen (TMP) crosslinking of plasmid pJ992. The extent of psoralen cross-linking was measured by plasmid isolation, restriction digestion, denaturation, electrophoresis and Southern blotting to measure the extent of crosslink-enabled rapid dsDNA renaturation. Sample autoradiograms are shown in Figure 3B, and the results of image quantitation are given in Figure 3C and Table 3. These data show that levels of unrestrained negative supercoiling in the WT and ΔHU backgrounds are similar, while negative supercoiling in ΔH-NS and ΔIHF strains was increased relative to WT (Table 3). These results generally track with measured levels of total supercoiling except for the ΔH-NS strain.

We found the TMP crosslinking assay to be technically challenging and only moderately reproducible for the present purpose. We therefore performed a more direct bioassay that has recently been reported for the measurement of unrestrained supercoiling in bacteria (61). This assay exploits the fact that the promoters driving expression of DNA gyrase (p*gyrA*) and topoisomerase I (p*topA*) are oppositely responsive to local levels of unrestrained negative supercoiling. The *gyrA* promoter is repressed by high unrestrained negative supercoiling and activated when unrestrained negative supercoiling is low. In contrast, the promoter cluster driving *topA* is activated by high unrestrained negative supercoiling and repressed when unrestrained negative supercoiling is low. This intuitively reasonable relationship supports bacterial supercoiling homeostasis. By placing reporter genes downstream from these promoters (Figure 4) in separate plasmid constructs or in the bacterial assay episome itself, the ratio of *topA*:*gyrA* reporter activities can be used to monitor unrestrained negative supercoiling *in vivo*. This assay approach was applied to WT, ΔHU, ΔIHF and ΔH-NS strains with reporter promoters either carried on high or low-copy number plasmids of different sizes or integrated into the large F′ episome, providing the results shown in Table 3. As seen for total supercoiling, the extent of unrestrained negative supercoiling was found to be very similar for WT and ΔH-NS strains, independent of the DNA construct carrying the reporters. This result was completely reproducible, though it does not agree with a previous report that loss of H-NS caused a modest increase in negative supercoiling (58). In contrast, the diagnostic *Qsc* ratio for ΔHU cells depended on the location of the reporter genes. For plasmids, the *Qsc* ratios were significantly less than the WT ratio, but the *Qsc* value was more variable and somewhat increased versus WT when assayed in the F′ episome (Table 3). The basis for context-dependent changes in the unrestrained negative supercoiling in the absence of HU protein is unknown. The data in Table 3 also show that unrestrained negative supercoiling was consistently and significantly higher in ΔIHF cells, with the diagnostic *Qsc* ratio 2- to 4-fold higher that observed for WT cells: for ΔIHF cells the results of all supercoiling assays are concordant.

Table 3. DNA supercoiling[a]

Strain	Total negative supercoiling (chloroquine titration)	Unrestrained negative supercoiling (% of control psoralen reactivity)	Unrestrained negative supercoiling (*Qsc* index)[b]	*Qsc* index (% of control)
WT	WT level (reference)	100[c]	2.1 ± 0.2[d]	100 ± 9[d]
			3.0 ± 0.3[e]	100 ± 9[e]
			3.1 ± 0.5[f]	100 ± 16[f]
ΔHU	Noticeable decrease	90[c]	0.7 ± 0.1[d]	34 ± 5[d]
			2.0 ± 0.3[e]	68 ± 10[e]
			5.9 ± 2.3[f]	190 ± 73[f]
ΔH-NS	Slight decrease	330[c]	2.2 ± 0.1[d]	102 ± 6[d]
			2.6 ± 0.2[e]	87 ± 6[e]
			3.2 ± 0.3[f]	101 ± 11[f]
ΔIHF	Large increase	560[c]	4.6 ± 0.2[d]	220 ± 7[d]
			13.7 ± 1.2[e]	455 ± 38[e]
			12.7 ± 2.3[f]	405 ± 73[f]

[a]Calculated as described in 'Materials and Methods' section based on rate of psoralen cross-linking or *topA*: *gyrA* ratios of reporter gene expression, where the promoters are inversely responsive to local unrestrained superhelical tension.
[b]Quotient of supercoiling, defined as *topA*: *gyrA* reporter ratio after normalization for cell density as described in 'Materials and Methods' section.
[c]Based on reactivity of plasmid pJ992.
[d]Based on *topA*: *gyrA* reporter ratio in large plasmids pJ1345 and pJ1346.
[e]Based on *topA*: *gyrA* reporter ratio in small plasmids pJ1454 and pJ1456.
[f]Based on *topA*: *gyrA* reporter ratio in the bacterial F′ episome.

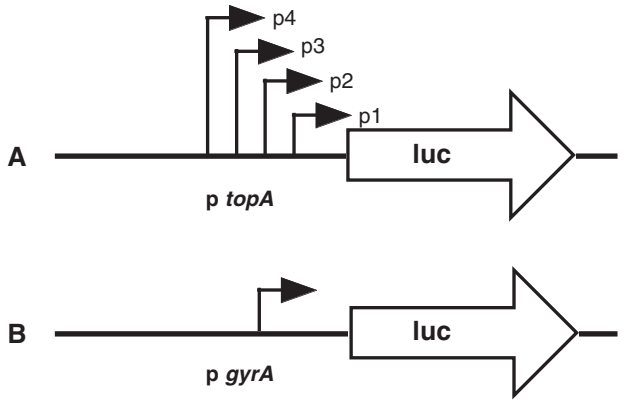

Figure 4. Schematic elements of promoter/reporter constructs for monitoring unrestrained supercoiling in *E. coli*. Constructs contain firefly luciferase reporters. (**A**) Luciferase expression is driven from the cluster of *topA* promoters, induced by high levels of negative superhelical strain and repressed by low levels of negative superhelical strain. (**B**) Luciferase expression is driven by the *gyrA* promoter, induced by low levels of negative supercoiling and repressed by high levels of negative supercoiling.

Three important conclusions can be drawn from these supercoiling assays. First, the promoter activity bioassays of unrestrained supercoiling in the test strains parallel the results of total supercoiling assays. In general it appears

that a fairly constant fraction of total supercoiling is due to unrestrained supercoiling *in vivo*. Second, unrestrained supercoiling estimates from supercoiling-dependent promoters generally do not depend on whether the promoter-reporters are present on plasmids or episomes. Third, and most importantly here, the effects of eliminating different nucleoid proteins on repression loop stability *cannot* be explained simply by invoking perturbations in local unrestrained supercoiling. Comparison of the data in Table 3 and Figure 2 reveal *no correlation* between repression loop stability and levels of unrestrained negative supercoiling in the different genetic backgrounds tested. In particular, ΔH-NS cells showed strongly enhanced DNA looping but had a level of negative DNA supercoiling that was similar to WT cells (Table 3). The ΔIHF cells showed strongly increased unrestrained negative supercoiling but little change in DNA looping (Table 3). The ΔHU cells have only slightly decreased negative supercoiling but show substantial changes in loop stability and character. These results suggest that the observed changes in looping are not caused by indirect supercoiling effects. This conclusion also supports our previous observation that DNA looping was not reduced when total negative supercoiling in *E. coli* was reduced using the gyrase inhibitor Norfloxacin (49).

Model for enhanced DNA looping in the absence of H-NS

The data in Figure 2 indicate that loss of the H-NS protein enhances the formation of the experimental DNA loop in living *E. coli*. The data in Figure 3 and Table 3 show that this effect does not involve changes in DNA supercoiling. How might the loss of H-NS facilitate DNA looping? Single molecule experiments have shown that H-NS, like other DNA-binding proteins (68,69), can either endow flexibility (at low binding densities) or stiffness (at high binding densities) (24,42). If H-NS concentrations were sufficient to drive high protein occupation of the repression loop, DNA stiffening might antagonize looping, but this seems unlikely, as exponentially growing cells are thought to contain only about one H-NS dimer per 1400 bp of DNA (21,70). Another model to explain H-NS inhibition of DNA looping is based on the observation that H-NS dimers have two DNA-binding domains and can bridge between DNA duplexes (21,43). Such cross-linking could inhibit DNA looping by the mechanism shown in Figure 5. Looping requires the shortening of a segment of DNA and would be inhibited if DNA segments are cross-linked by H-NS proteins and not free to slide past one another in the crowded nucleoid.

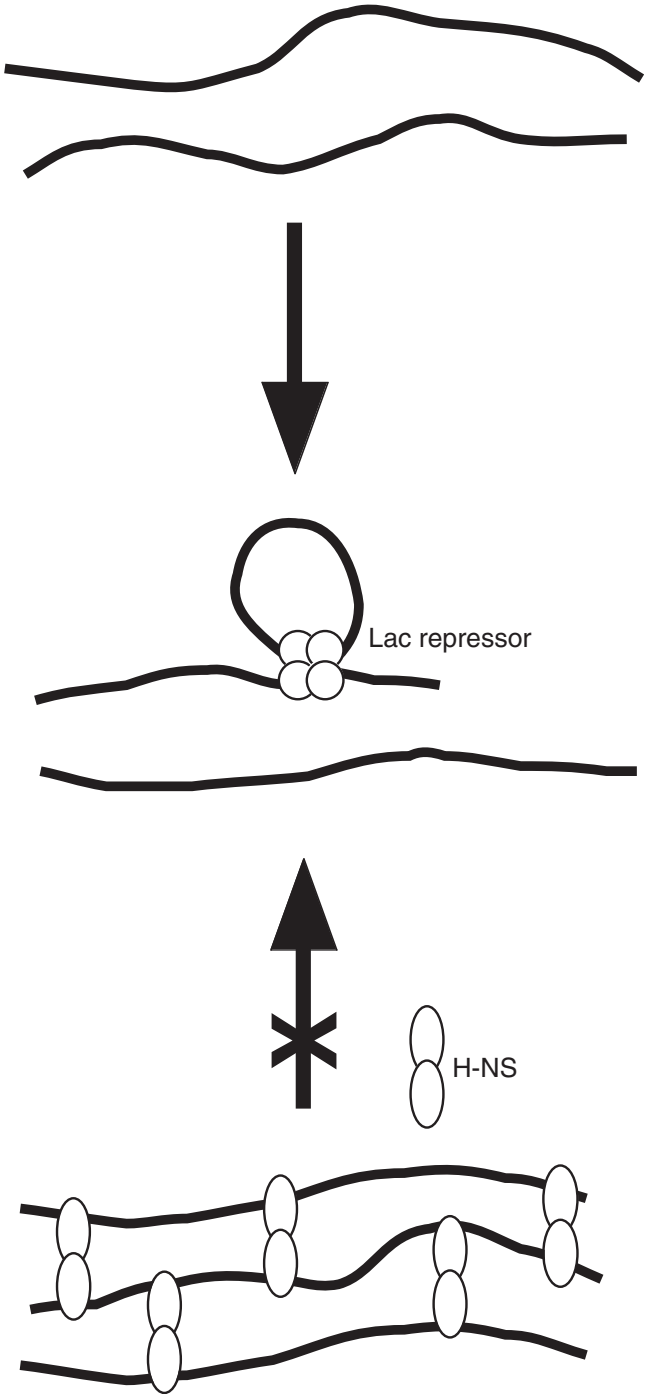

Figure 5. Model for DNA looping inhibition by H-NS protein. DNA looping in one DNA molecule requires it to freely slide past another nearby DNA (upper arrow). If the nearby DNA strands are extensively cross-linked by bidentate H-NS dimers (open ovals), DNA looping may be inhibited.

SUMMARY AND IMPLICATIONS

We have adapted classic work on the *lac* operon (45–48) to develop a system for studying *in vivo* DNA flexibility. Regulatory elements from the *lac* operon have been organized into a series of episomal constructs in which reporter gene repression is highly dependent on the stability of a small DNA loop between operators. We previously used this system to show that DNA twist inflexibility limits looping *in vivo*, while optimal loop stabilities are independent of DNA length over the range 63–91 bp (49). We also demonstrated weak DNA looping by Lac repressor even when saturated by IPTG, and showed evidence that loss of the nucleoid protein HU destabilized repression loops. The present experiments confirm and extend these conclusions. We demonstrate

that the simple statistical weights/DNA mechanics model used here can capture the observed experimental variations and suggest underlying physical interpretations. It has not been necessary to include explicit consideration of DNA bending persistence length changes or alternative loop shapes, but the lack of a DNA length effect and the calculated values of the torsional modulus confirm that the apparent effective flexibility of DNA *in vivo* is much greater than would be expected from *in vitro* experiments.

The structure and composition of the bacterial nucleoid is ill-defined, and much remains to be learned regarding the roles of major nucleoid proteins. In one proposed classification (21), nucleoid proteins are characterized as DNA bridging factors (H-NS, SMC, Lrp) or DNA bending factors (HU, IHF, Fis). Our study used DNA loop stabilization as a probe of the effects of HU, IHF and H-NS proteins on properties of the *E. coli* nucleoid. We conclude that loss of the sequence-non-specific DNA bending factor HU strongly destabilizes a repression loop, while loss of the sequence-specific bending factor IHF has much less effect. In contrast, loss of the DNA bridging factor H-NS from the nucleoid *facilitates* DNA looping. We show that the effects of these gene disruptions on DNA looping do not generally correlate with their effects on negative DNA supercoiling in the host. We therefore interpret the DNA looping phenotypes of HU, IHF and H-NS deletion strains as evidence for direct protein–DNA interactions that alter the apparent physical properties of the looped DNA. We cannot rule out that DNA looping effects observed upon removing nucleoid proteins could have more complex origins. For example, mutant strains may express altered levels of the remaining nucleoid proteins and/or other factors related to apparent DNA flexibility (39). The different effects on DNA looping of IHF versus HU loss may be due to the lower abundance of IHF or to higher non-sequence-dependent DNA binding by HU in the DNA loop. Future studies will investigate whether IHF and HU participate in the experimental repression loop. The strong enhancement of DNA looping upon deletion of H-NS is surprising, and the mechanism remains unknown. It remains possible that the loss of H-NS might simply reduce competition for important HU sites near the DNA loop, but we suggest that loop stabilization is due to inhibition of DNA slithering. Comparisons among other bending and bridging proteins should resolve this issue.

SUPPLEMENTARY DATA

Supplementary Data are available at NAR Online.

ACKNOWLEDGEMENTS

We gratefully acknowledge molecular constructs, strains, advice and discussion from F. Whipple, P. Heisig, R. Sinden, R. Phillips, L. Bintu, S. Levene and G. Koudelka. Support was received from the Mayo Foundation and from NIH grants GM54411 and GM075965 (L.J.M.). This work was supported by the Mayo Foundation and by NIH Grants GM054411 and GM075965 to L.J.M. Funding to pay the Open Access publication charges for the article was provided by National Institutes of Health.

Conflict of interest statement. None declared.

REFERENCES

1. Garcia,H.G., Grayson,P., Han,L., Inamdar,M., Kondev,J., Nelson,P.C., Phillips,R., Widom,J. and Wiggins,P.A. (2007) Biological consequences of tightly bent DNA: the other life of a macromolecular celebrity. *Biopolymers*, **85**, 115–130.
2. Cloutier,T.E. and Widom,J. (2004) Spontaneous sharp bending of double-stranded DNA. *Mol. Cell*, **14**, 355–362.
3. Cloutier,T.E. and Widom,J. (2005) DNA twisting flexibility and the formation of sharply looped protein-DNA complexes. *Proc. Natl Acad. Sci. USA*, **102**, 3645–3650.
4. Du,Q., Smith,C., Shiffeldrim,N., Vologodskaia,M. and Vologodskii,A. (2005) Cyclization of short DNA fragments and bending fluctuations of the double helix. *Proc. Natl Acad. Sci. USA*, **102**, 5397–5402.
5. Maher,L.J.3rd. (2006) DNA kinks available…if needed. *Structure*, **14**, 1479–1480.
6. Wiggins,P.A., Van Der Heijden,T., Moreno-Herrero,F., Spakowitz,A., Phillips,R., Widom,J., Dekker,C. and Nelson,P.C. (2006) High flexibility of DNA on short length scales probed by atomic force microscopy. *Nature Nanotech.*, **1**, 137–141.
7. Paull,T.T., Haykinson,M.J. and Johnson,R.C. (1993) The nonspecific DNA-binding and -bending proteins HMG1 and HMG2 promote the assembly of complex nucleoprotein structures. *Genes Dev.*, **7**, 1521–1534.
8. Ross,E.D., Hardwidge,P.R. and Maher,L.J.3rd. (2001) HMG proteins and DNA flexibility in transcription activation. *Mol. Cell. Biol.*, **21**, 6598–6605.
9. Crothers,D.M. (1993) Architectural elements in nucleoprotein complexes. *Curr. Biol.*, **3**, 675–676.
10. Pontiggia,A., Rimini,R., Harley,V.R., Goodfellow,P.N., Lovell-Badge,R. and Bianchi,M.E. (1994) Sex-reversing mutations affect the architecture of SRY-DNA complexes. *EMBO J.*, **13**, 6115–6124.
11. Travers,A.A., Ner,S.S. and Churchill,M.E.A. (1994) DNA chaperones: a solution to a persistence problem. *Cell*, **77**, 167–169.
12. Wolffe,A.P. (1994) Architectural transcription factors. *Science*, **264**, 1100–1101.
13. Churchill,M.E., Jones,D.N., Glaser,T., Hefner,H., Searles,M.A. and Travers,A.A. (1995) HMG-D is an architecture-specific protein that preferentially binds to DNA containing the dinucleotide TG. *EMBO J.*, **14**, 1264–1275.
14. Love,J.J., Li,X., Case,D.A., Giese,K., Grosschedl,R. and Wright,P.E. (1995) Structural basis for DNA bending by the architectural transcription factor LEF-1. *Nature*, **376**, 791–795.
15. Bustin,M. and Reeves,R. (1996) High-mobility-group chromosomal proteins: architectural components that facilitate chromatin function. *Prog. Nucleic Acid Res. Mol. Biol.*, **54**, 35–100.
16. Werner,M.H., Gronenborn,A.M. and Clore,G.M. (1996) Intercalation, DNA kinking, and the control of transcription. *Science*, **271**, 778–784.
17. Werner,M.H. and Burley,S.K. (1997) Architectural transcription factors: proteins that remodel DNA. *Cell*, **88**, 733–736.
18. Ellwood,K.B., Yen,Y.M., Johnson,R.C. and Carey,M. (2000) Mechanism for specificity by HMG-1 in enhanceosome assembly. *Mol. Cell. Biol.*, **20**, 4359–4370.
19. Mitsouras,K., Wong,B., Arayata,C., Johnson,R.C. and Carey,M. (2002) The DNA architectural protein HMGB1 displays two distinct modes of action that promote enhanceosome assembly. *Mol. Cell. Biol.*, **22**, 4390–4401.
20. Swinger,K.K. and Rice,P.A. (2004) IHF and HU: flexible architects of bent DNA. *Curr. Opin. Struct. Biol.*, **14**, 28–35.
21. Luijsterburg,M.S., Noom,M.C., Wuite,G.J.L. and Dame,R.T. (2006) The architectural role of nucleoid-associated proteins in the organization of bacterial chromatin: a molecular perspective. *J. Struct. Biol.*, **156**, 262–272.

22. Azam,T.A. and Ishihama,A. (1999) Twelve species of the nucleoid-associated protein from Escherichia coli. Sequence recognition specificity and DNA binding affinity. *J. Biol. Chem.*, **274**, 33105–33113.
23. McLeod,S.M. and Johnson,R.C. (2001) Control of transcription by nucleoid proteins. *Curr. Opin. Microbiol.*, **4**, 152–159.
24. Dame,R.T. and Goosen,N. (2002) HU: promoting or counteracting DNA compaction? *FEBS Lett.*, **529**, 151–156.
25. Bianchi,M.E. (1994) Prokaryotic HU and eukaryotic HMG1: a kinked relationship. *Mol. Microbiol.*, **14**, 1–5.
26. Bianchi,M.E., Beltrame,M. and Paonessa,G. (1989) Specific recognition of cruciform DNA by nuclear protein HMG1. *Science*, **243**, 1056–1059.
27. Bonnefoy,E., Takahashi,M. and Yaniv,J.R. (1994) DNA-binding parameters of the HU protein of *Escherichia coli* to cruciform DNA. *J. Mol. Biol.*, **242**, 116–129.
28. Pontiggia,A., Negri,A., Beltrame,M. and Bianchi,M.E. (1993) Protein HU binds specifically to kinked DNA. *Mol. Microbiol.*, **7**, 343–350.
29. Lewis,D.E., Geanacopoulos,M. and Adhya,S. (1999) Role of HU and DNA supercoiling in transcription repression: specialized nucleoprotein repression complex at gal promoters in Escherichia coli. *Mol. Microbiol.*, **31**, 451–461.
30. Swinger,K.K., Lemberg,K.M., Zhang,Y. and Rice,P.A. (2003) Flexible DNA bending in HU-DNA cocrystal structures. *EMBO J.*, **22**, 3749–3760.
31. Rice,P.A., Yang,S., Mizuuchi,K. and Nash,H.A. (1996) Crystal structure of an IHF-DNA complex: a protein-induced DNA U-turn. *Cell*, **87**, 1295–1306.
32. Travers,A. (1997) DNA-protein interactions: IHF–the master bender. *Curr. Biol.*, **7**, R252–R254.
33. Rice,P.A. (1997) Making DNA do a U-turn: IHF and related proteins. *Curr. Opin. Struct. Biol.*, **7**, 86–93.
34. Zulianello,L., de la Gorgue de Rosny,E., van Ulsen,P., van de Putte,P. and Goosen,N. (1994) The HimA and HimD subunits of integration host factor can specifically bind to DNA as homodimers. *EMBO J.*, **13**, 1534–1540.
35. Arfin,S.M., Long,A.D., Ito,E.T., Tolleri,L., Riehle,M.M., Paegle,E.S. and Hatfield,G.W. (2000) Global gene expression profiling in Escherichia coli K12. The effects of integration host factor. *J. Biol. Chem.*, **275**, 29672–29684.
36. Azam,T.A., Hiraga,S. and Ishihama,A. (2000) Two types of localization of the DNA-binding proteins within the Escherichia coli nucleoid. *Genes Cells*, **5**, 613–626.
37. Dorman,C.J. (2004) H-NS: a universal regulator for a dynamic genome. *Nat. Rev. Microbiol.*, **2**, 391–400.
38. Smyth,C.P., Lundback,T., Renzoni,D., Siligardi,G., Beavil,R., Layton,M., Sidebotham,J.M., Hinton,J.C., Driscoll,P.C. *et al.* (2000) Oligomerization of the chromatin-structuring protein H-NS. *Mol. Microbiol.*, **36**, 962–972.
39. Brescia,C.C., Kaw,M.K. and Sledjeski,D.D. (2004) The DNA binding protein H-NS binds to and alters the stability of RNA in vitro and in vivo. *J. Mol. Biol.*, **339**, 505–514.
40. Dame,R.T., Wyman,C. and Goosen,N. (2000) H-NS mediated compaction of DNA visualised by atomic force microscopy. *Nucleic Acids Res.*, **28**, 3504–3510.
41. Dame,R.T., Wyman,C. and Goosen,N. (2001) Structural basis for preferential binding of H-NS to curved DNA. *Biochimie*, **83**, 231–234.
42. Dame,R.T. and Wuite,G.J. (2003) On the role of H-NS in the organization of bacterial chromatin: from bulk to single molecules and back. *Biophys. J.*, **85**, 4146–4148.
43. Dame,R.T., Luijsterburg,M.S., Krin,E., Bertin,P.N., Wagner,R. and Wuite,G.J. (2005) DNA bridging: a property shared among H-NS-like proteins. *J. Bacteriol.*, **187**, 1845–1848.
44. Doyle,M., Fookes,M., Ivens,A., Mangan,M.W., Wain,J. and Dorman,C.J. (2007) An H-NS-like stealth protein aids horizontal DNA transmission in bacteria. *Science*, **315**, 251–252.
45. Mossing,M.C. and Record,M.T.Jr. (1986) Upstream operators enhance repression of the *lac* promoter. *Science*, **233**, 889–892.
46. Bellomy,G., Mossing,M. and Record,M. (1988) Physical properties of DNA *in vivo* as probed by the length dependence of the *lac* operator looping process. *Biochemistry*, **27**, 3900–3906.
47. Law,S.M., Bellomy,G.R., Schlax,P.J. and Record,M.T.Jr. (1993) In vivo thermodynamic analysis of repression with and without looping in lac constructs. Estimates of free and local lac repressor concentrations and of physical properties of a region of supercoiled plasmid DNA in vivo. *J. Mol. Biol.*, **230**, 161–173.
48. Muller,J., Oehler,S. and Müller-Hill,B. (1996) Repression of lac promoter as a function of distance, phase and quality of an auxiliary lac operator. *J. Mol. Biol.*, **257**, 21–29.
49. Becker,N.A., Kahn,J.D. and Maher,L.J.3rd. (2005) Bacterial repression loops require enhanced DNA flexibility. *J. Mol. Biol.*, **349**, 716–730.
50. Zhang,Y., McEwen,A.E., Crothers,D.M. and Levene,S.D. (2006) Analysis of in-vivo LacR-mediated gene repression based on the mechanics of DNA looping. *PLoS ONE*, **1**, e136.
51. Swigon,D., Coleman,B.D. and Olson,W.K. (2006) Modeling the Lac repressor-operator assembly: the influence of DNA looping on Lac repressor conformation. *Proc. Natl Acad. Sci. USA*, **103**, 9879–9884.
52. Mehta,R.A. and Kahn,J.D. (1999) Designed hyperstable Lac repressor•DNA loop topologies suggest alternative loop geometries. *J. Mol. Biol.*, **294**, 67–77.
53. Saiz,L., Rubi,J.M. and Vilar,J.M. (2005) Inferring the in vivo looping properties of DNA. *Proc. Natl Acad. Sci. USA*, **102**, 17642–17645.
54. Whipple,F.W. (1998) Genetic analysis of prokaryotic and eukaryotic DNA-binding proteins in *Escherichia coli*. *Nucleic Acids Res.*, **26**, 3700–3706.
55. Datsenko,K.A. and Wanner,B.L. (2000) One-step inactivation of chromosomal genes in Escherichia coli K-12 using PCR products. *Proc. Natl Acad. Sci. USA*, **97**, 6640–6645.
56. Miller,J. (1992) *A Short Course in Bacterial Genetics*. Cold Spring Harbor Laboratory Press, New York.
57. Zechiedrich,E.L., Khodursky,A.B., Bachellier,S., Schneider,R., Chen,D., Lilley,D.M. and Cozzarelli,N.R. (2000) Roles of topoisomerases in maintaining steady-state DNA supercoiling in Escherichia coli. *J. Biol. Chem.*, **275**, 8103–8113.
58. Mojica,F.J. and Higgins,C.F. (1997) In vivo supercoiling of plasmid and chromosomal DNA in an Escherichia coli hns mutant. *J. Bacteriol.*, **179**, 3528–3533.
59. Sinden,R.R. and Ussery,D.W. (1992) Analysis of DNA structure in vivo using psoralen photobinding: measurement of supercoiling, topological domains, and DNA-protein interactions. *Methods Enzymol.*, **212**, 319–335.
60. Cook,D.N., Armstrong,G.A. and Hearst,J.E. (1989) Induction of anaerobic gene expression in Rhodobacter capsulatus is not accompanied by a local change in chromosomal supercoiling as measured by a novel assay. *J. Bacteriol.*, **171**, 4836–4843.
61. Preisler,A., Mraheil,M.A. and Heisig,P. (2006) Role of novel gyrA mutations in the suppression of the fluoroquinolone resistance genotype of vaccine strain Salmonella Typhimurium vacT (gyrA D87G). *J. Antimicrob. Chemother.*, **57**, 430–436.
62. Aki,T. and Adhya,S. (1997) Repressor induced site-specific binding of HU for transcriptional regulation. *EMBO J.*, **16**, 3666–3674.
63. Drlica,K. (1992) Control of bacterial DNA supercoiling. *Mol. Microbiol.*, **6**, 425–433.
64. Boroweic,J.A., Zhang,L., Sasse-Dwight,S. and Gralla,J.D. (1987) DNA supercoiling promotes formation of a bent repression loop in *lac* DNA. *J. Mol. Biol.*, **196**, 101–111.
65. Kramer,H., Amouyal,M., Nordheim,A. and Müller-Hill,B. (1988) DNA supercoiling changes the spacing requirements of two lac operators for DNA loop formation with lac repressor. *EMBO J.*, **7**, 547–556.
66. Lia,G., Bensimon,D., Croquette,V., Allemand,J.F., Dunlap,D., Lewis,D.E., Adhya,S. and Finzi,L. (2003) Supercoiling and denaturation in Gal repressor/heat unstable nucleoid protein (HU)-mediated DNA looping. *Proc. Natl Acad. Sci. USA*, **100**, 11373–11377.

67. Kramer,P.R. and Sinden,R.R. (1997) Measurement of unrestrained negative supercoiling and topological domain size in living human cells. *Biochemistry*, **36**, 3151–3158.
68. Van Noort,J., Verbrugge,S., Goosen,N., Dekker,C. and Dame,R.T. (2004) Dual architectural roles of HU: formation of flexible hinges and rigid filaments. *Proc. Natl Acad. Sci. USA*, **101**, 6969–6974.
69. McCauley,M., Hardwidge,P.R., Maher,L.J.3rd and Williams,M.C. (2005) Dual binding modes for an HMG domain from human HMGB2 on DNA. *Biophys. J.*, **89**, 353–364.
70. Ali Azam,T., Iwata,A., Nishimura,A., Ueda,S. and Ishihama,A. (1999) Growth phase-dependent variation in protein composition of the Escherichia coli nucleoid. *J. Bacteriol.*, **181**, 6361–6370.